J1.2 Short-term wind forecasting at the Hong Kong International Airport by applying chaotic oscillatory-based neural network to LIDAR data

K.M. Kwong
Hong Kong Polytechnic University, Hong Kong, China

P.W. Chan *
Hong Kong Observatory, Hong Kong, China

1. INTRODUCTION

Short-term forecasting of the wind within the next half to one hour or so is useful in the provision of meteorological services for a localized area, such as aviation weather service. Situated at a coastal area with complex terrain, wind forecasting for the Hong Kong International Airport (HKIA) is very challenging. The wind distribution could change rapidly due to terrain disruption of the background airflow. Land-sea interaction also results in the onset and retreat of sea breeze in the vicinity of HKIA in fine weather. Besides the choice of runways for aircraft landing/departing, short-term forecasting of the wind could enhance the provision of low-level windshear and turbulence warning services.

Szeto and Chan (2006) studied the possibility of forecasting the wind field at the airport area in the short term using a numerical weather prediction (NWP) model. This approach involves the ingestion of a vast amount of meteorological observations, both within and outside the airport area, into the model and numerical integration of the future states of the atmosphere following a set of thermodynamic and dynamic equations of atmospheric variables. This paper considers an alternative approach, namely, training a neural network (NN) based on the past wind data in the airport area at high spatial resolution and using the NN to make short-term forecasting of the wind. The basic philosophy is that, if we are just interested in the future evolution of the wind field in a short period of time, e.g. the next half an hour, it may be sufficient to consider the correlation between the winds at various locations around the airport as a quasi-closed physical system, i.e. without involving the wind and the other meteorological elements outside the system, such as the "background" wind and temperature profiles measured at locations far away from the airport. This approach is similar to short-term wind forecasting by extrapolation of the main features of the wind field at the airport, but should be more sophisticated because it involves NN training of the past data. On the other hand, the application of NWP models for such short-term forecasting of the wind may have limitations due to the initial spin-up required to balance the various meteorological variables and large demand for computational resources.

Doppler LIght Detection And Ranging (LIDAR) systems are operated by the Hong Kong Observatory (HKO) at HKIA for windshear and turbulence alerting. They measure the winds up to 10 km away at high spatial resolutions. The surveillance scans typically have a resolution of 105 m in range and about 1 degree in azimuth. The radial velocity data from one of the LIDARs at HKIA (namely, the one situated near the middle of the airfield at a height of 50 m AMSL) would be used in this study. The NN and the LIDAR data used in this study are described in Section 2. As a start, the NN is used to forecast the next surveillance scan result after 6 minutes, as described in Section 3. Then the method is extended for wind forecasting up to 30 minutes, and the results are presented in Section 4. The conclusions of the study are drawn in Section 5.

* *Corresponding author address:* P.W. Chan, Hong Kong Observatory, 134A Nathan Road, Hong Kong email: pwchan@hko.gov.hk

2. NEURAL NETWORK AND THE LIDAR DATA

2.1 Chaotic oscillator

The idea of chaotic neural networks was proposed by Aihara, Takabe and Toyoda (1990). They stated that in neurophysiology viewpoint real neuron operations are more complex than simple thresholding. Therefore non-linear output function is more suitable to act as activate function of a neuron. They developed chaotic neural networks to model non-linear behaviour of a neuron.

Details of chaotic oscillatory-based neural network (CONN) and Lee oscillator could be found in Lee (2004) and Lee and Wong (2007). Only a summary of CONN is given here. Research on neuroscience and brain science in this couple of years discovered that there are various chaotic phenomena in brain functions such as oscillation between excitatory and inhibitory neurons. From these findings, a kind of artificial neural network, namely, CONN, and various models to simulate human's neural behaviour have been developed. One of these models is the Lee oscillator. The Lee oscillator contains the neural dynamics of four constitutive neural elements: *u*, *v*, *w* and *z*. The neural dynamics are given by:

$$u(t+1) = f[a_1 \cdot u(t) - a_2 \cdot v(t) + I(t) - \theta_u] \quad (1)$$

$$v(t+1) = f[b_1 \cdot u(t) - b_2 \cdot v(t) - \theta_v] \quad (2)$$

$$w(t+1) = f[I(t)] \quad (3)$$

$$z(t) = f[u(t) - v(t)] \cdot e^{-kI^2(t)} + w(t) \quad (4)$$

where *u(t)*, *v(t)*, *w(t)*, and *z(t)* are the state variables of the excitatory, inhibitory, input, and output neurons, respectively; *f()* is the hyperbolic tangent function; a_1, a_2, b_1, and b_2 are the weight parameters for these constitutive neurons; θ_u and θ_v are the thresholds for excitatory and inhibitory neurons; *I(t)*is the external input stimulus; and *k* is the decay constant. Figure 1 shows the bifurcation behaviour of Lee oscillator model.

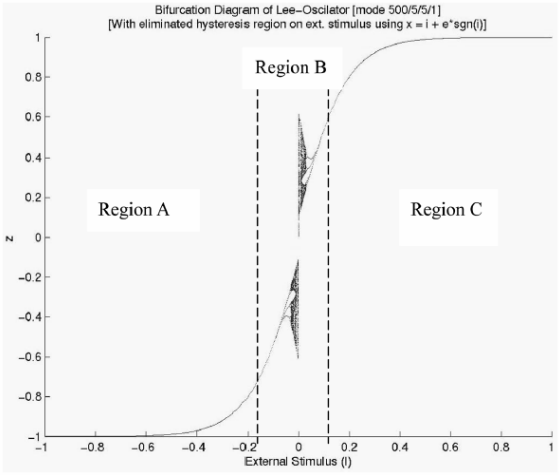

Figure 1 Bifurcation diagram of Lee oscillator.

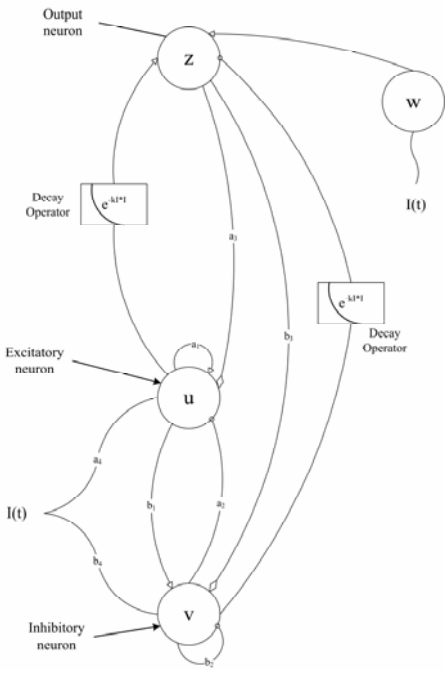

Figure 2 Lee oscillator (retrograde transport) model.

The Lee oscillator is enhanced according to the retrograde transport mechanism in axons (Lee and Wong, 2007). The neural dynamics are given by:

$$u(t+1) = f[a_1 \cdot u(t) - a_2 \cdot v(t) + a_3 \cdot z(t) + a_4 \cdot I(t) - \theta_u] \quad (5)$$

$$v(t+1) = f[b_3 \cdot z(t) - b_1 \cdot u(t) - b_2 \cdot v(t) + b_4 \cdot I(t) - \theta_v] \quad (6)$$

$$w(t+1) = f[I(t)] \quad (7)$$

$$z(t) = f[v(t) - u(t)] \cdot e^{-kI^2(t)} + w(t) \quad (8)$$

and represented schematically in Figure 2. There are three major amendments from the original Lee oscillator. Firstly, the recycling concept of the axon's retrograde transport is implemented by including *z(t)* in both excitatory neuron (Eq. (5)) and inhibitory neuron (Eq. (6)). Secondly, *I(t)* is included in Eq. (6) because incoming signal should also be considered in inhibitory neuron. Thirdly, new parameters a_3, a_4, b_3, b_4 were added in Eq. (5) and (6), so that every variable has its own parameter to adjust the outcomes.

2.2 System framework of CONN

The CONN is the core part of the forecasting model. Its structure is essentially a backpropagation neural network, but with the neurons replaced by the Lee oscillator (retrograde transport) model having different parameter settings instead of the conventional sigmoid function. The structure is given by (Lee and Wong, 2007):

$$y_k = f_{lee}\left[\sum_j w_{kj} f_{lee}\left(\sum_i v_{ji} x_i\right)\right] \quad (9)$$

where x_i are the input values; y_k are output values,; weights connecting the input layer unit *i* and the hidden layer unit *j* are denoted by v_{ji}; weights connecting the hidden layer unit *j* and the output layer unit *k* are designated as w_{kj}; and f_{lee} is the Lee oscillator with different parameters in each neuron.

Two different parameter settings of the Lee oscillator (retrograde transport) model are used. As shown schematically in Figure 3, neurons with the two parameter settings are used in the hidden layer alternatively, whereas only one parameter setting is adopted in the output layer. Based on a previous study (Lee and Wong, 2007), the oscillation of a single setting in CONN may be too strong or too weak, and the use of two parameter settings for the Lee oscillator in the hidden layer appears to balance the oscillation power at a proper level. Further research would be required to study in greater depth the characteristics of chaotic oscillators with different parameters and to arrange them in a more balanced way.

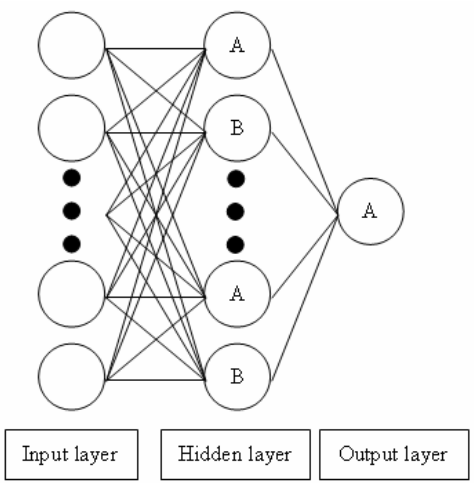

Figure 3 Structure of the CONN in the present study.

2.3 Preparation of the LIDAR data

The LIDAR's radial velocity data in the surveillance scans at 1-degree elevation are employed in this study. They are first processed by the quality control algorithm described in Chan et al. (2006). For a particular location in the surveillance scan with missing data, if valid velocity data are available at the neighbouring positions, its velocity

value is provided by bilinear interpolation (in range and in azimuth) of the velocities at the neighbouring points. The radial velocities are normalized (to between -1 and 1) before being used in the training of the CONN. Likewise, for forecasting by CONN, the past velocities are normalized first, and the predicted values are denormalized and plotted.

3. FORECASTING FOR 6 MINUTES

As discussed in Section 1, it is assumed in the present study that, over a very short time interval (6-30 minutes), the future evolution of the wind at a location is related to the wind distribution in its vicinity. As such, for each data point in the LIDAR's sector scan, a relationship is built up between the velocity at this point and those at the 5 x 5 neighbouring points around (i.e. about 500 m in the radial direction and 5 degrees in the azimuth centred at the data point under consideration) through training of the CONN. Due to the large amount of velocity data but limited availability of computing power, the training is performed using the data in the last 2 hours only. The training of the neural network is shown schematically in Figure 4. For every 6 minutes, the actual velocity distribution (depicted in blue) is used to make a 6-minute forecast. The weighting parameters inside the neural network are tuned so that the forecast is as close to the reality (depicted in yellow) as possible. The process is repeated for 2 hours, and the weighting parameters inside the neural network are continuously adjusted.

After the training for 2 hours' data, the LIDAR data are used to make a forecast into the future distribution of the radial velocity. As shown in Figure 4, the LIDAR data of 24 minutes are employed (i.e. the 102nd minute to 126th minute) to the make the forecast in the next 6 minutes (i.e. the 132nd minute). The forecast wind field is given in red in Figure 4. The process is repeated. For each 6-minute forecast wind field, a total of 15 individual forecasts are made from the previous 24 minutes by using slightly different weighing parameters of the neural network (which are generated by random). At every location in the LIDAR's sector scan area, the two extreme velocity values (i.e. the highest normalized velocity and the lowest normalized velocity) are removed, and the remaining 13 velocity values are averaged to give the final 6-minute forecast value. This "ensemble average" approach helps suppress the noise in the velocity field from the individual forecast.

Two case studies have been conducted for this 6-minute forecast. The first example is given in Figure 5. It is a case of the emergence of mountain wake flow to the southwest of HKIA on 20 July 2006. The forecast wind field basically captures the occurrence of the mountain wake, with slight reverse flow (winds blowing towards the LIDAR as coloured in green vs. the prevailing flow blowing away from the LIDAR as coloured in brown).

Another example is shown in Figure 6. It is the retreat of a sea breeze front in the late afternoon of 26 October 2006. In general, the neural network forecast gives the trend of the occurrence of easterly wind (coloured brown in Figure 6) over the western part of HKIA. However, the area of the westerly sea breeze (coloured green in Figure 6) is overestimated.

4. FORECASTING FOR 30 MINUTES

The methodology described in Section 3 is extended to make forecast for 30 minutes. The training of the neural network and the forecasting based on the trained network are shown schematically in Figure 7. Five wind distributions (depicted in blue) are used to forecast the winds in the next 30 minutes, and the weighting parameters in the neural network are adjusted by comparing with the reality (yellow). After training for about 2 hours, the latest 24 minutes' data are used to give a forecast of the next 30 minutes (depicted in red).

The results for the mountain wake case on 20 July 2006 are shown in Figure 8(a). The trend of the occurrence of the wake flow is successfully captured, though the areal extent of the wake is over-estimated. To quantitatively assess the similarity between the forecast and the actual wind distributions, root-mean-square (RMS) error of the forecast field is computed. As a control, the RMS error of the persistence method is also evaluated, namely, using the last wind distribution in the 24-minute input dataset as a "forecast" of the wind distribution in the next 30 minutes. As given in Figure 8(b), neural network outperforms the persistence method for the last 12 minutes or so in the 30-minute forecast period.

The case of retreating sea breeze is shown in Figure 9(a). The neural network forecast successfully captures the trend of the spreading of away-from-the-LIDAR flow (yellow and brown) to the northwest over western part of HKIA, though the rate of spreading is slower than reality. It has smaller RMS error compared to persistence except in the last 6 minutes of the 30-minute forecast period.

5. CONCLUSIONS

To the knowledge of the authors, the present work is the first application of CONN to 2D wind forecasting based on LIDAR. Due to limitation in computing resources, only the wind data of 2 hours or so are used in the training of the neural network, which is definitely not sufficient to cover all the complicated wind patterns that could occur in the vicinity of HKIA due to weather phenomena as diverse as mountain wake flow, mountain waves, sea breeze, etc. Despite this limitation, based on two case studies, the methodology at least shows skills in capturing the trend of the occurrence of mountain wake flow and the retreating of sea breeze. For 30-minute forecast, the RMS error could be lower than that from the simple rule of persistence.

Future work would focus on the training of the neural network using a much larger dataset (at least a couple of months) but with a reduced area for the wind forecast. For instance, instead of a 2D wind distribution, only the 1D wind variation along a glide path of HKIA is considered. The wind forecast for the glide path would be useful in the short-term alerting of low-level windshear (Chan et al. 2006).

References

Aihara K., T.Takabe, and M. Toyoda, 1990: Chaotic neural networks. *Physical Letters A*, **144(6)**, 333-340.

Chan, P.W., C.M. Shun and K.C. Wu, 2006: Operational LIDAR-based system for automatic windshear alerting at the Hong Kong International Airport. *12th Conference on Aviation, Range, and Aerospace Meteorology*, American Meteorological Society.

Lee, R.S.T., 2004: A transient-chaotic auto-associative network (TCAN) based on Lee oscillators. *IEEE Transaction on Neural Network*, **15(5)**, 1228-1243.

Lee, R.S.T., and M.H.Y. Wong, 2007: Wind shear forecasting by chaotic oscillatory-based neural networks (CONN) with Lee Oscillator (retrograde transport) model. Submitted to *IEEE Transaction on Neural Network*.

Szeto, K.C., and P.W. Chan, 2006: High resolution numerical modelling of windshear episodes at the Hong Kong International Airport. *12th Conference on Aviation, Range, and Aerospace Meteorology*, American Meteorological Society.

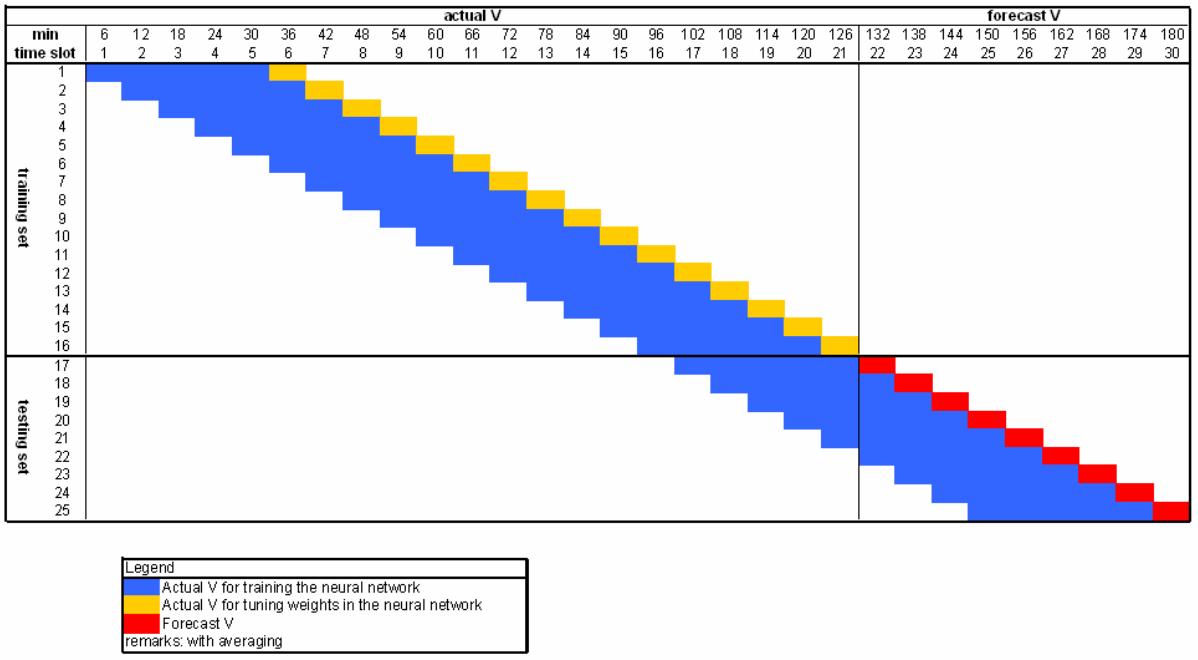

Figure 4 Schematic diagram showing the data used for training the neural network and forecasting the wind field in the next 6 minutes (the next LIDAR scan).

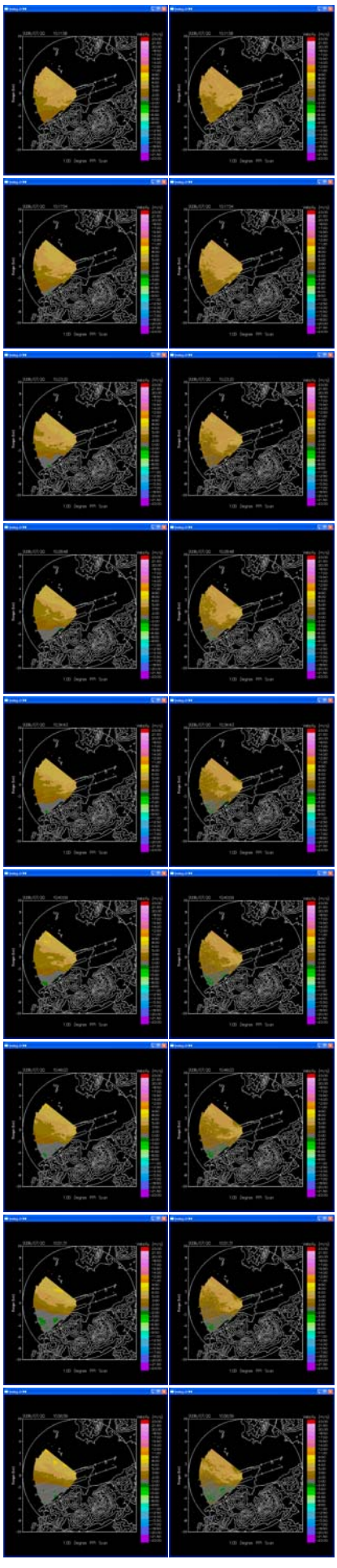

Figure 5 Mountain wake case in easterly wind: actual LIDAR observations separated by 6 minutes (left) and the corresponding 6-minute forecast by the neural network (right).

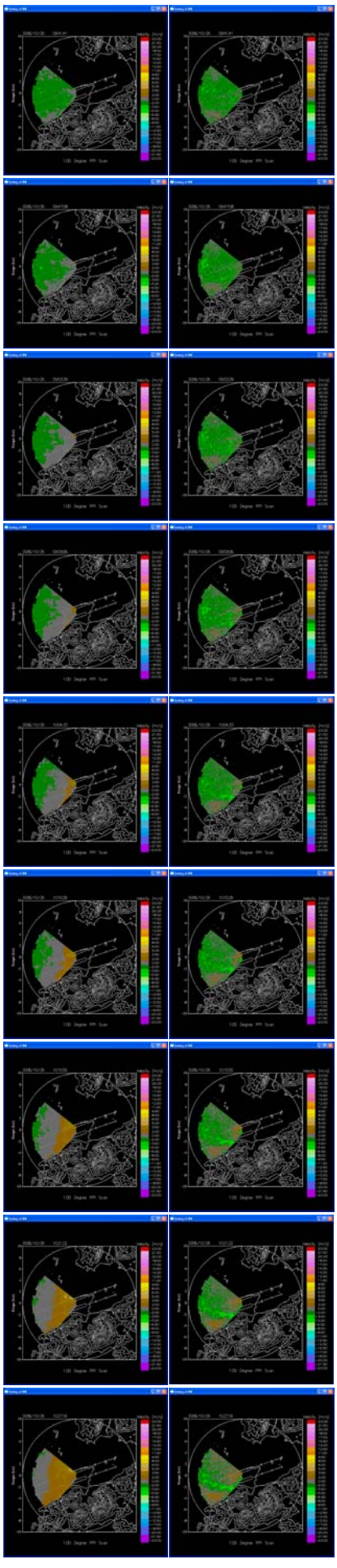

Figure 6 The case of retreating westerly sea breeze and the establishment of the prevailing easterly wind over the airport: actual LIDAR observations separated by 6 minutes (left) and the corresponding 6-minute forecast by the neural network (right).

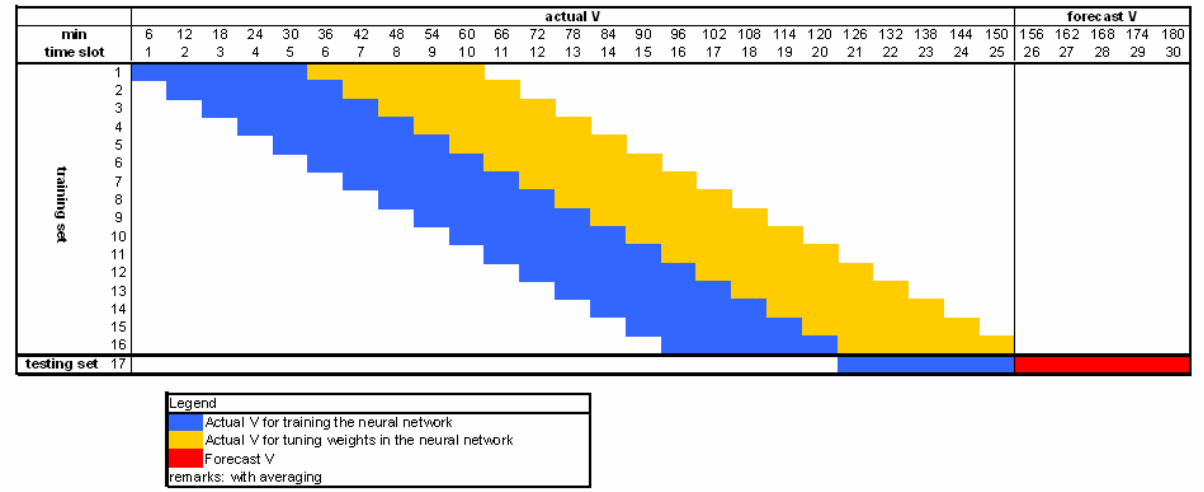

Figure 7 Schematic diagram showing the data used for training the neural network and forecasting the wind field in the next 30 minutes (the next 5 LIDAR scans).

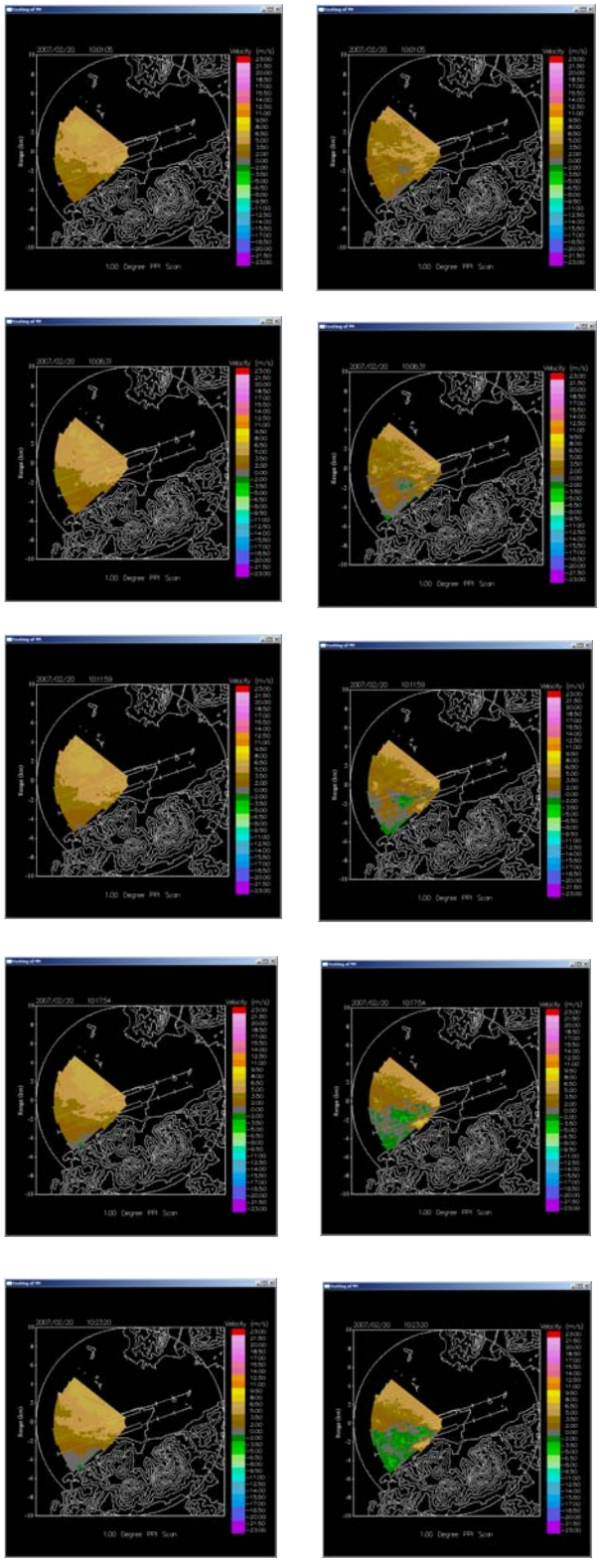

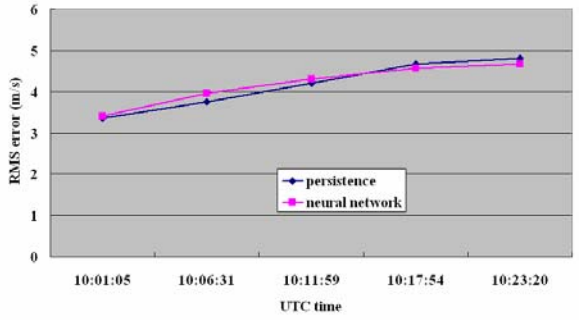

Figure 8 Similar to Figure 5, but for 30-minute forecast using the neural network. The RMS errors of the persistence method and the neural network are shown in the graphs above.

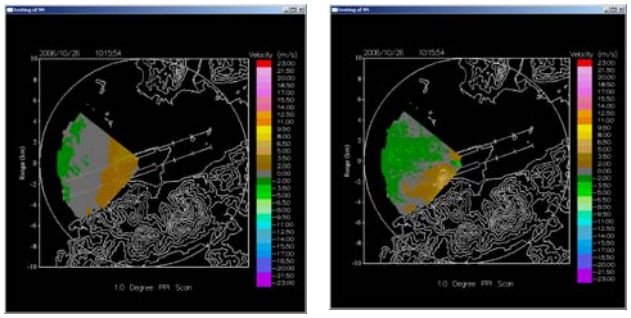

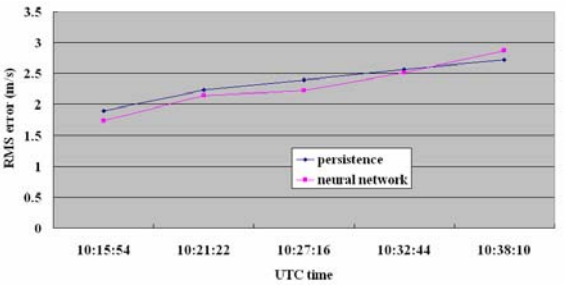

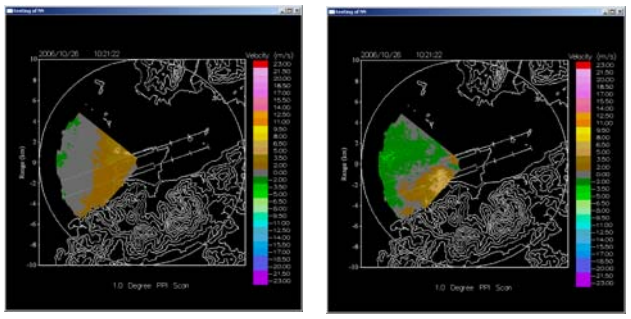

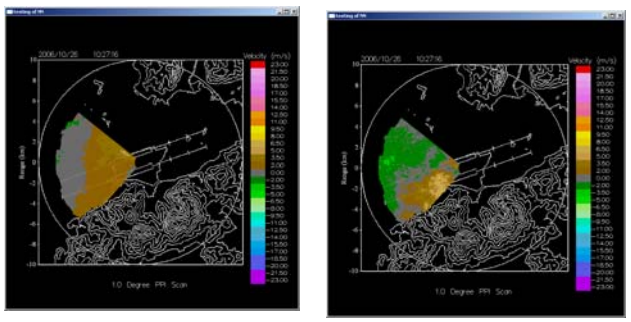

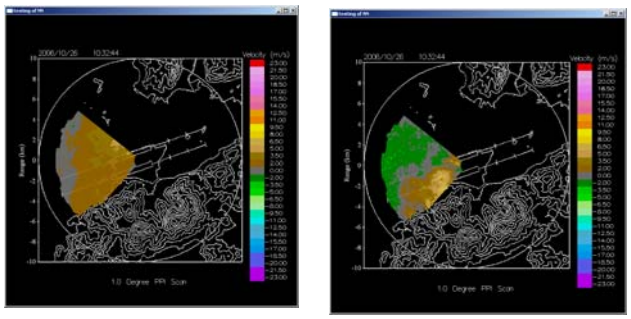

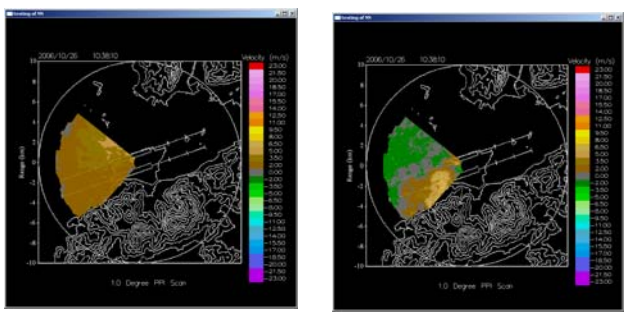

Figure 9 Similar to Figure 6, but for 30-minute forecast using the neural network. The RMS errors of the persistence method and the neural network are shown in the graphs above.